دليل المؤتمر السوري - الفرنسي الأول للطاقات المتجددة

دمشق 24-28 تشرين الأول (أكتوبر) 2010

CFSER 2010

PARAMETRIC TORSIONAL VIBRATIONS OF A DRIVE TRAIN IN HORIZONTAL AXIS WIND TURBINE

Michael Todorov [a], Georgi Vukov [b]

[a] Department of Aeronautics, Technical University of Sofia, Sofia

[b] Department of Applied Mechanics, University of Forestry Engineering, Sofia

michael.todorov@tu-sofia.bg

Abstract

The authors propose here a dynamic multi-body model of a wind turbine which includes a rotor, a drive train and an electrical generator. The drive train has a three-stage gearbox which contains two high-speed parallel gear stages and a low-speed planetary gear stage. The model consists of 10 bodies and has 11 degrees of freedom. The model takes into account the stiffness of the engaged tooth pairs as time functions. In this model the aerodynamic and generator torques are applied as external loads. The calculation permits to obtain time series of torsional vibrations and amplitude-frequency characteristics for an industrial wind turbine. The results show that transient loads in the gearbox have complex character and require special attention. The modeling can be used for fault and wear gear diagnostic.

Key Words : wind turbine, drive train, vibrations

1. Introduction

The wind energy application has been growing rapidly for the last few years. In the last ten years the global installed capacity of wind energy has increased 20 times. This trend is expected to continue in Europe. The increase in the rotor and hence size of the turbine leads to a complicated design of the drive train in the wind turbine beside higher requirements of turbine reliability.

Design calculations for a wind turbine base on simulation of mechanical loads on the turbine components caused by external forces. The external forces are the wind, the electricity grid and sea waves for offshore applications.

The multi-body simulation techniques are used to analyze the loads on internal components of drive trains. The simplest model with one degree of freedom (DOF) for each drive train component is used to investigate only torsional vibrations in the drive train. In this model all bodies have one DOF, i.e. the rotation around their axis of symmetry. Therefore, the coupling of two bodies involves 2 DOF's. Gear contact forces between two wheels are modeled with a linear spring acting in the plane of action along the contact line (normal to the tooth surface). This modeling is valid for heavily and moderately loaded gears, Minchev et Grigorov [1998], Kahraman [1993]. More complex model with 6 DOF's for each drive train component is used

for investigation of the influence of bearing stiffness on the internal dynamics of the drive train. All drive train components are treated as rigid bodies. The linkages in the multi-body model, representing the bearing and tooth flexibilities, have 12 DOF's, Parey et al. [2006], Vedmar et Andersson [2003]. Finally, it is used a flexible model in which the drive train components are modeled as finite element models instead of rigid bodies, Ambarisha et Parker [2006], Andersson et Vedmar [2003], Lundvall et al. [2004], Vinayak et Singh [1998]. This model adds a possibility of calculating stress and deformation in the drive train components in some time. Any addition to the model leads to additional information about dynamics of the drive train but makes the modeling and the simulation more complicated. Litak et Friswell [2004], Parey et al. [2006], Wojnarowski et Onishchenko [2003], Yuksel et Kahraman [2004] present the effects of the tooth defects and the wearing on the gear dynamics.

The modern wind turbines have a planetary gearbox. Studies on the vibrations in a planetary gear system have been done by Ambarisha et Parker [2006], Dresig et Schreiber [2005], Khang et al. [2004], Lin et Parker, [1999], [2002], [2007], Parker [2008], Theodossiades et Natsiavas [2001]. The tooth meshes are modeled as a linear spring with stiffness which is a time function. For this reason the vibration equations of a planetary gear system are differential equations with periodic coefficients, Ambarisha et Parker [2006], Khang et al. [2004], Lin et Parker [1999], [2002], [2007], Theodossiades et Natsiavas [2001].

The applications of these modeling techniques on different drive trains of wind turbines are presented in Gold et al. [2004], Heege [2003], [2007], Peeters et al. [2002], [2004], [2006], Peeters [2006], Rosas [2003], Shlecht et Shulze [2003], [2006], Shlecht et al. [2004], Sørensen et al. [2003], VOITH [2006]. Different simulations for specific wind turbines are presented in Ekanayake et al. [2003], Fuglseth [2005], Hansen et al. [2002], Ramtharan et al. [2007], Shi et al. [2007], Sørensen et al. [2003]. Todorov et al. [2007], [2009] present the numerical investigations for the given wind turbine in this paper, where the meshes stiffness are modeled as constant springs. In this case the differential equations, which describe the torsional vibrations of the wind turbine, have constant coefficients.

2. Dynamic model of the wind turbine

The wind turbine consists of a rotor, a drive train and a generator (Fig.1). The drive train has a gearbox with three stages. The gear stages include two high-speed parallel gear stages (helical

gear pairs) and a low-speed planetary gear stage (three identical planets with spur teeth, sun and fixed ring wheel) (Fig.2).

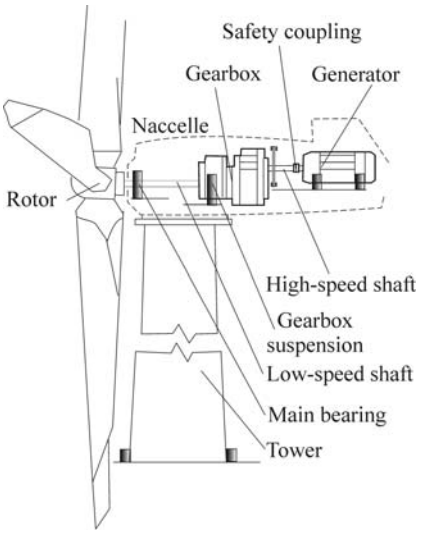

Fig. 1. *Schematic sketch of wind turbine*

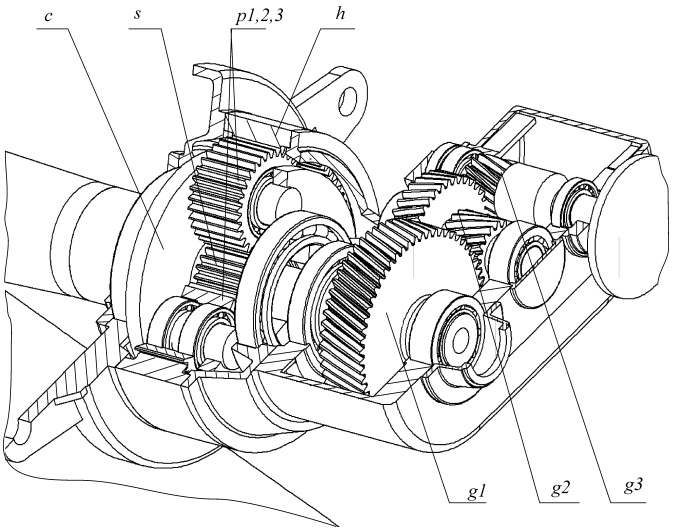

Fig. 2. *Sketch of gearbox: h-hull, c-carrier, p1,2,3-planets, s-sun, g1,2,3-gears*

The dynamic multi-body model is shown in Fig.3. It consists of a rotor with 3 rigid blades, a low-speed elastic shaft, a gearbox with 3 gear stages, a high-speed elastic shaft and a generator rotor. Thus, the model consists of 10 bodies and 11 DOF's.

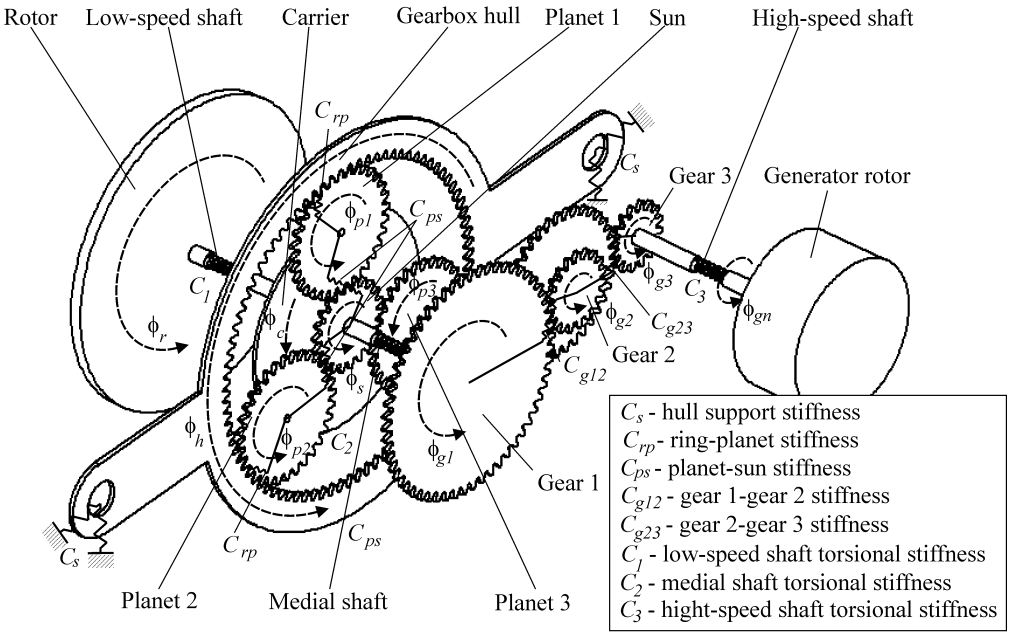

Fig. 3. *Dynamical model of wind turbine*

The gear contact forces between wheels are modeled by linear spring acting in the plane of action along the contact line (normal to the tooth surface), Veits et al. [1984], Minchev et Grigorov [1998], Zakrajesek [1989]. The stiffness gear is defined as a normal distributed tooth force in a normal plane causing the deformation of one or more engaging tooth pairs, over a distance of 1 μm, normal to a envolvent profile in a normal plane, Deutsches Institut für Normung [1987]. This deformation results from the bending of the teeth in contact between the two gear wheels, the one of which is fixed and the other is loaded. The stiffness varies in the time and can be expressed in a time Fourier series form, Khang et al. [2004], Lin et Parker [2002], [2007], Theodossiades et Natsiavas [2001]. For instance,

$$C_{g_i}(t) = C_{g_i} + C_{g_{i_v}}(t)$$

where C_{g_i} and $C_{g_i v}$ are mean and time-varying components of the stiffness. The variation part is periodic with frequency $\Omega_i = z_i \omega_i$ (z_i is the number of teeth on the gears, ω_i is mean angular velocity of the gear shafts) and it is expressed in Fourier series as

$$C_{g_{i_v}}(t) = 2C_{g_i} \sum_{s=1}^{\infty} \left(a_s \sin s\Omega_i t + b_s \cos s\Omega_i t\right)$$

where

$$a_s = -\frac{2}{s\pi} \sin\left[s\pi(\varepsilon - 2p)\right] \sin(s\pi\varepsilon)$$

$$b_s = -\frac{2}{s\pi} \cos\left[s\pi(\varepsilon - 2p)\right] \sin(s\pi\varepsilon)$$

Without loss of generality, it can be accepted that $p = 0$ (p is the phasing between planets) Lin et Parker [2002]. In practice, three or four Fourier terms reasonably approximate the stiffness variation.

Damping and friction forces are not included. These assumptions are valid for heavily to moderately loaded gears that are correctly for a large wind turbine, Kahraman [1993], Minchev et Grigorov [1998].

It is also accepted that the masses of the planets are identical.

In this article Lagrange's equations are used to obtain the equations of the torsional vibrations of the wind turbine, Amirouche [2006], Coutinho [2001], Nikravesh [1988], Shabana [2005], Wittenburg [1977]. The vector of the generalized co-ordinates is

$$\{q\} = \begin{bmatrix} \phi_h & \phi_c & \phi_r & \phi_{p1} & \phi_{p2} & \phi_{p3} & \phi_s & \phi_{g1} & \phi_{g2} & \phi_{g3} & \phi_{gn} \end{bmatrix}^T$$

where ϕ_i (i=h,c,r,p1,p2,p3,s,g1,g2,g3,gn) are the rotational angles of the ring (gearbox hull), carrier, rotor (hub), planet 1, planet 2, planet 3, sun, gear 1, gear 2, gear 3 and the generator rotor (Fig. 3).

The differential equations, describing the torsional vibrations of the wind turbine, are

$$[M]\{\ddot{q}\} + [C(t) - \omega^2 C_\omega]\{q\} = \{T\},$$

where M is the inertia matrix and C is the stiffness matrix. The matrix C_ω results from the carrier rotation.

The vector of the external forces, caused by the wind and the electricity grid, is

$$\{T\} = \begin{bmatrix} 0 & 0 & T_{aero} & 0 & 0 & 0 & 0 & 0 & 0 & 0 & T_{gen} \end{bmatrix}^T,$$

where T_{aero} and T_{gen} are the aerodynamic and electromagnetic torques.

The non-zero numbers of inertia matrix M are

$$m_{1,1} = J_h + J_c + m_c l_{cr}^2 + J_r + m_r l_{cr}^2 + 3J_p + 3m_p l_{cr}^2 + 3m_p r_c^2 + J_s + m_s l_{cr}^2 + I_{g1} + m_{g1} l_{g12}^2 + \\ + I_{g2} + m_{g2} l_{g22}^2 + I_{g3} + m_{g3} l_{g23}^2;$$

$$m_{1,2} = m_{2,1} = J_c + J_r + 3J_p + 3m_p r_c^2;$$

$$m_{1,3} = m_{3,1} = m_{2,3} = m_{3,2} = m_{3,3} = J_r;$$

$$m_{1,4} = m_{4,1} = m_{1,5} = m_{1,6} = m_{6,1} = m_{5,1} = m_{2,4} = m_{4,2} = m_{2,5} = m_{5,2} = m_{2,6} = m_{6,2} = m_{4,4} = \\ = m_{5,5} = m_{6,6} = I_p;$$

$$m_{1,7} = m_{7,1} = m_{7,7} = I_s;\ m_{1,8} = m_{8,1} = m_{8,8} = I_{g1};\ m_{1,9} = m_{9,1} = m_{9,9} = I_{g2};$$

$$m_{1,10} = m_{10,1} = m_{10,10} = I_{g3};\ m_{2,2} = J_c + J_r + 3J_p + 3m_p r_c^2;\ m_{11,11} = I_{gn}.$$

The non-zero numbers of stiffness matrix C are

$$c_{1,1} = C_{s1}\left(l_{s1}^2 + l_{s2}^2\right) + C_{rp}(t)\left(3r_R^2 + 3r_c^2 + 3r_p^2 - 6r_R r_c\right) + C_{ps}(t)\left(3r_c^2 + 3r_p^2 + 3r_s^2 - 6r_c r_s \cos\alpha\right) + \\ + C_{g12}(t)\left(l_{g12} - l_{g22}\right)^2 + C_{g23}(t)\left(l_{g22} - l_{g23}\right)^2;$$

$$c_{1,2} = c_{2,1} = C_{rp}(t)\left(3r_c^2 + 3r_p^2 - 3r_R r_c\right) + C_{ps}(t)\left(3r_c^2 + 3r_p^2 - 3r_c r_s \cos\alpha\right);$$

$$c_{1,4} = c_{4,1} = C_{rp}(t)\left[r_p^2 - r_R r_p \cos(\omega t + \alpha) + r_c r_p \cos(\omega t + \alpha)\right] +$$
$$+ C_{ps}(t)\left[r_p^2 - r_c r_p \cos(\omega t - \alpha) + r_s r_p \cos\omega t\right];$$

$$c_{1,5} = c_{5,1} = C_{rp}(t)\left[r_p^2 + r_R r_p \cos(60 - \omega t - \alpha) - r_c r_p \cos(60 - \omega t - \alpha)\right] +$$
$$+ C_{ps}(t)\left[r_p^2 + r_c r_p \cos(60 - \omega t + \alpha) - r_s r_p \cos(60 - \omega t)\right];$$

$$c_{1,6} = c_{6,1} = C_{rp}(t)\left[r_p^2 + r_R r_p \cos(60 + \omega t + \alpha) - r_c r_p \cos(60 + \omega t + \alpha)\right] +$$
$$+ C_{ps}(t)\left[r_p^2 + r_c r_p \cos(60 + \omega t - \alpha) - r_s r_p \cos(60 + \omega t)\right];$$

$$c_{1,7} = c_{7,1} = C_{ps}(t)\left(3r_s^2 - r_c r_s \cos\alpha\right);\ \ c_{1,8} = c_{8,1} = C_{g12}(t) r_{g1}\left(l_{g12} - l_{g22}\right)\cos\alpha\cos\beta;$$

$$c_{1,9} = c_{9,1} = C_{g12}(t) r_{g21}\left(l_{g12} - l_{g22}\right)\cos\alpha\cos\beta + C_{g23}(t) r_{g22}\left(l_{g22} - l_{g23}\right)\cos\alpha\cos\beta;$$

$$c_{1,10} = c_{10,1} = C_{g23}(t) r_{g3}\left(l_{g22} - l_{g23}\right)\cos\alpha\cos\beta;$$

$$c_{2,2} = C_{rr}(t)\left(3r_c^2 + 3r_p^2\right) + C_{ps}(t)\left(3r_c^2 + 3r_p^2\right);$$

$$c_{2,3} = -c_{3,3} = -C_1;\ \ c_{2,4} = c_{4,2} = C_{rp}(t)\left[r_p^2 + r_c r_p \cos(\omega t + \alpha)\right] + C_{ps}(t)\left[r_p^2 - r_c r_p \cos(\omega t - \alpha)\right];$$

$$c_{2,5} = c_{5,2} = C_{rp}(t)\left[r_p^2 - r_c r_p \cos(60 - \omega t - \alpha)\right] + C_{ps}(t)\left[r_p^2 + r_c r_p \cos(60 - \omega t + \alpha)\right];$$

$$c_{2,6} = c_{6,2} = C_{rp}(t)\left[r_p^2 - r_c r_p \cos(60 + \omega t + \alpha)\right] + C_{ps}(t)\left[r_p^2 + r_c r_p \cos(60 + \omega t - \alpha)\right];$$

$$c_{2,7} = c_{7,2} = -3C_{ps}(t) r_c r_s \cos\alpha;\ \ c_{4,4} = c_{5,5} = c_{6,6} = C_{rp}(t) r_p^2 + C_{ps}(t) r_p^2;$$

$$c_{4,7} = c_{7,4} = C_{ps}(t) r_s r_p \cos\omega t;\ \ c_{5,7} = c_{7,5} = -C_{ps}(t) r_s r_p \cos(60 - \omega t);$$

$$c_{6,7} = c_{7,6} = -C_{ps}(t) r_s r_p \cos(60 + \omega t);\ \ c_{7,7} = C_2 + 3C_{ps}(t) r_s^2;\ \ c_{7,8} = -C_2;$$

$$c_{8,8} = C_2 + C_{g12}(t) r_{g1}^2\left(\cos^2\alpha\cos^2\beta + \sin^2\alpha\right);\ \ c_{8,9} = C_{g12}(t) r_{g21}^2\left(\cos^2\alpha\cos^2\beta + \sin^2\alpha\right);$$

$$c_{9,9} = \left(C_{g12}(t) r_{g21}^2 + C_{g23}(t) r_{g22}^2\right)\left(\cos^2\alpha\cos^2\beta + \sin^2\alpha\right);$$

$$c_{9,10} = C_{g23}(t) r_{g22} r_{g3}\left(\cos^2\alpha\cos^2\beta + \sin^2\alpha\right);$$

$$c_{10,10} = C_3 + C_{g23}(t) r_{g3}^2\left(\cos^2\alpha\cos^2\beta + \sin^2\alpha\right);$$

$c_{10,11} = -c_{11,11} = -C_3$

The non-zero number of C_ω is

$c_{\omega_{2,2}} = 3m_p r_c^2$.

3. Results

The drive train data is listed in Table I. It is also assumed that the aerodynamic torque and electromagnetic torque are $T_{aero} = -T_{gen} =$ 15000 Nm. The rotor is turned with angular velocity $\omega = 18$ tr/min. The mesh stiffness between gears is shown in fig.5.

Table 1. *Drive Train Data*

J_h -inertia of the hull (kg·m^2)	473
J_c -inertia of the carrier (kg·m^2)	58
m_c - mass of the carrier (kg)	786
J_r - inertia of the rotor (kg·m^2)	$1.57 \cdot 10^6$
m_r - mass of the rotor (kg·m^2)	4144
J_p -inertia of the planets (kg·m^2)	1.12
m_p -mass of the planets (kg)	58
J_s -inertia of the sun (kg·m^2)	0.86
m_s -mass of the sun (kg)	146
J_{g1} -inertia of the gear 1 (kg·m^2)	14
m_{g1} -mass of the gear 1 (kg)	429
J_{g2} -inertia of the gear 2 (kg·m^2)	2.09
m_{g2} -mass of the gear 2 (kg)	159
J_{g3} -inertia of the gear 3 (kg·m^2)	1.27
m_{g3} -mass of the gear 3 (kg)	134
J_{gn} -inertia of the generator (kg·m^2)	93.22
C_1 -stiffness of the low-speed shaft (Nm/rad)	$7.19 \cdot 10^7$
C_2 -stiffness of the internal shaft (Nm/rad)	$1.40 \cdot 10^7$
C_3 -stiffness of the high-speed shaft (Nm/rad)	$0.15 \cdot 10^7$
C_{rp} -mean stiffness of the engaging tooth pairs ring-planets in the low-speed planetary gear stage (N/m)	$0.73 \cdot 10^8$
C_{ps} -mean stiffness of the engaging tooth pairs planets-sun in the low-speed planetary gear stage (N/m)	$0.73 \cdot 10^8$
C_{g12} -mean stiffness of the engaging tooth pairs in the 1st high-speed parallel gear stage (N/m)	$2.02 \cdot 10^9$

C_{g23} -mean stiffness of the engaging tooth pairs in the 2nd high-speed parallel gear stage (N/m)	$0.11 \cdot 10^8$
r_R - ring radius (mm)	420
r_c - carrier radius (mm)	270
r_p - planets radius (mm)	160
r_s - sun radius (mm)	110
r_{g1} - radius of gear 1 (mm)	290
r_{g21} - radius of gear 2 from the 2nd stage (mm)	95
r_{g22} - radius of gear 2 from the 3rd stage (mm)	185
r_{g3} - radius of gear 3 (mm)	80
l_{cr} -distance between hull center of gravity and centers of gravity of rotor, carrier, and sun (mm)	-130
l_{g12} -distance between hull center of gravity and center of gravity of gear 1 (mm)	-130
l_{g22} -distance between hull center of gravity and center of gravity of gear 2 (mm)	277
l_{g23} -distance between hull center of gravity and center of gravity of gear 3 (mm)	557
l_{s1} -distance between hull center of gravity and hull support (see fig.4) (mm)	-1282
l_{s2} -distance between hull center of gravity and hull support (see fig.4) (mm)	468
ε_{rp} -ring-planet contact ratio	1.9342
ε_{ps} -planet-sun contact ratio	1.6242
ε_{g12} -contact ratio of gears the 1st high-speed parallel gear stage	1.6616
ε_{g23} -contact ratio of gears the 2nd high-speed parallel gear stage	1.5984
α - pressure angle (°)	20
β - helix angle (°)	20
gear ratio	34.654

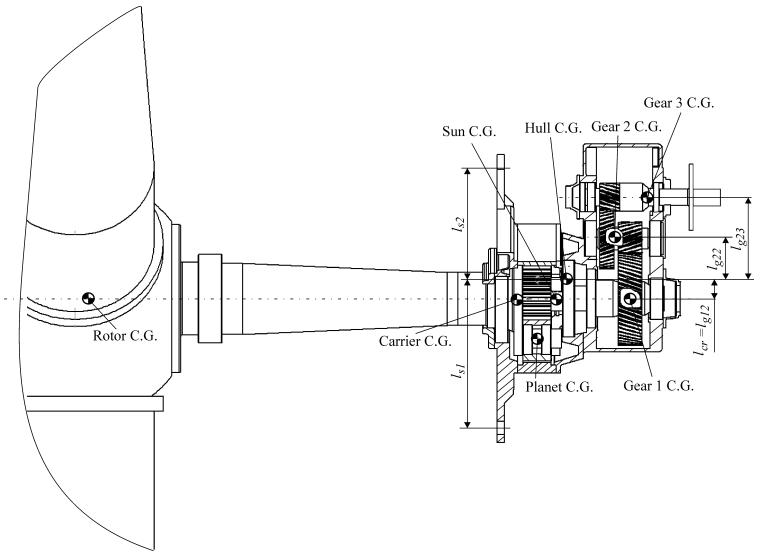

Fig.4

The results are shown in Fig.6-16.

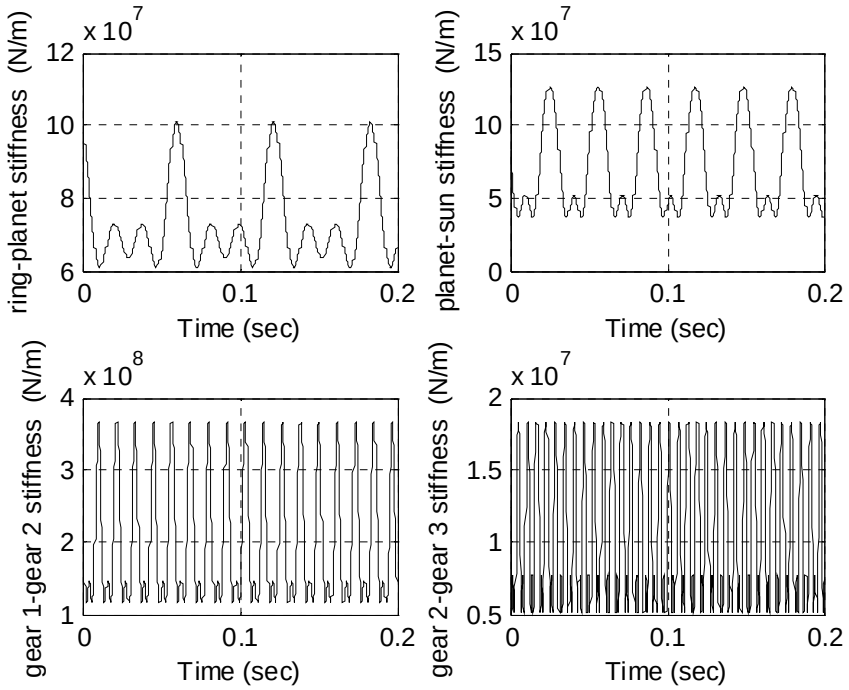

Fig. 5. *Mesh gears stiffness*

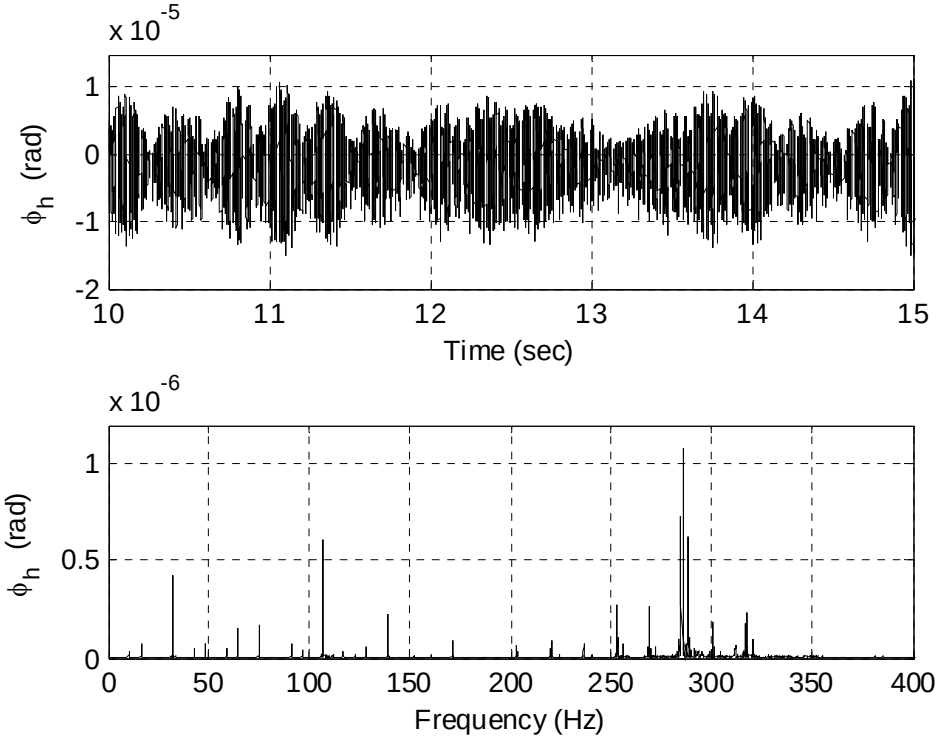

Fig. 6. *Hull rotational angle* ϕ_h. *From top: time series, amplitude-frequency characteristic*

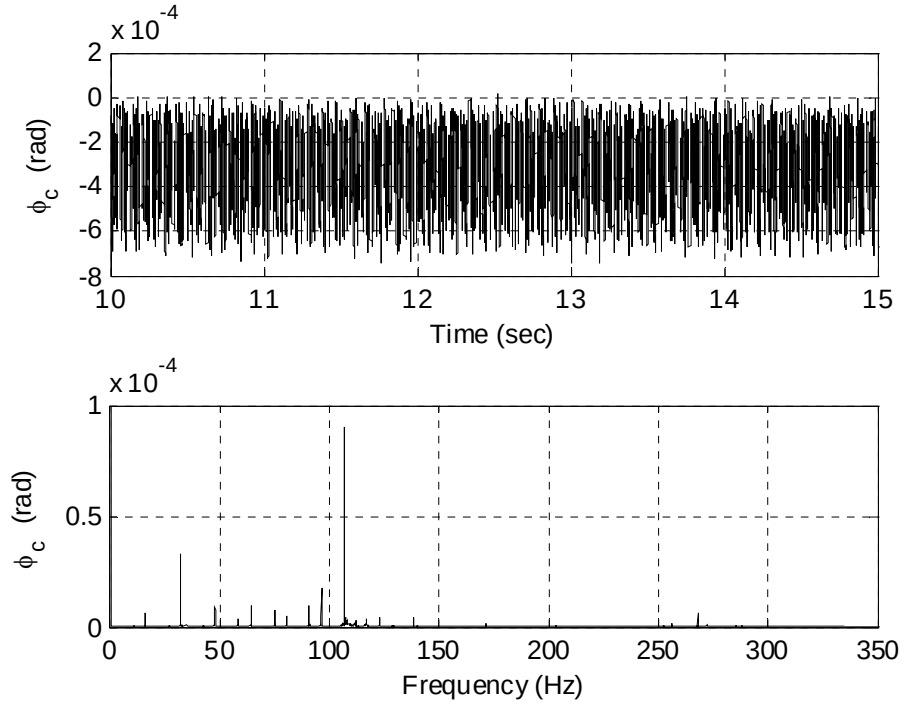

Fig. 7. *Carrier rotational angle* ϕ_c *. From top: time series, amplitude-frequency characteristic*

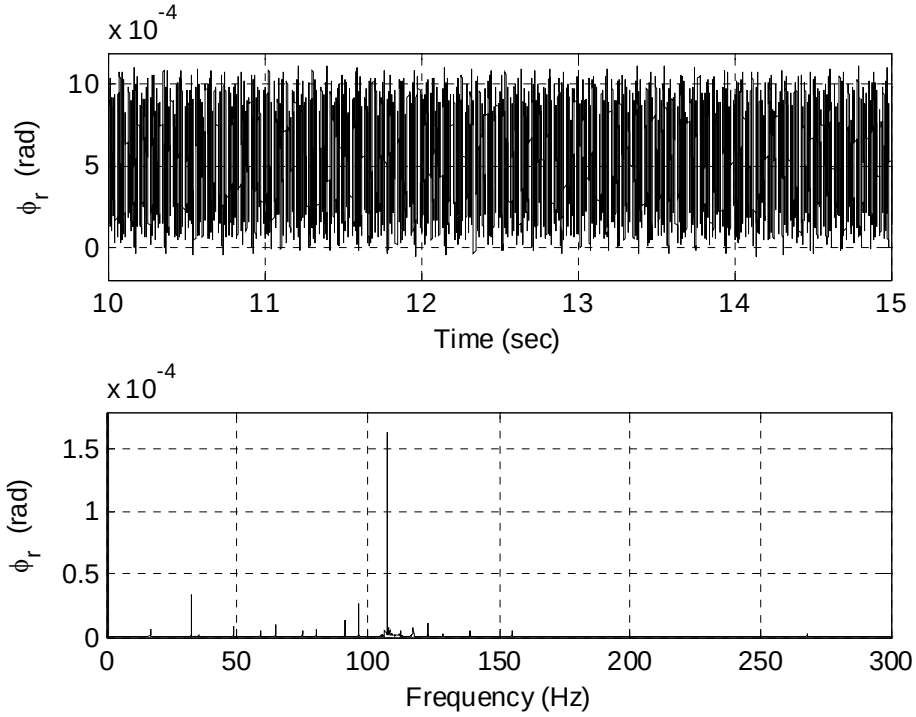

Fig. 8. *Rotor rotational angle* ϕ_r *. From top: time series, amplitude-frequency characteristic*

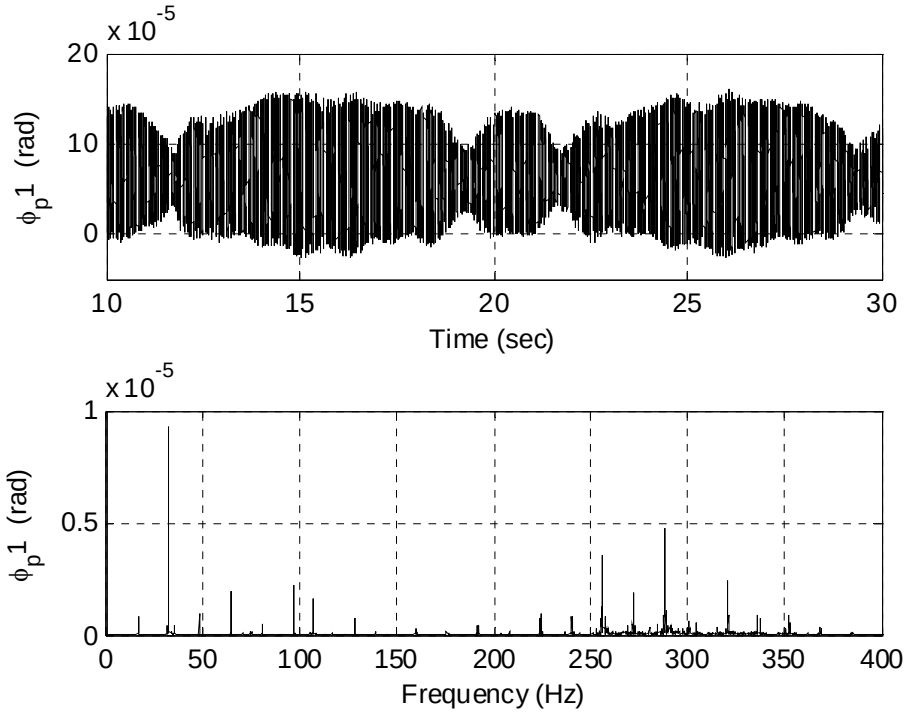

Fig. 9. *Planet 1 rotational angle* ϕ_{p1}. *From top: time series, amplitude-frequency characteristic*

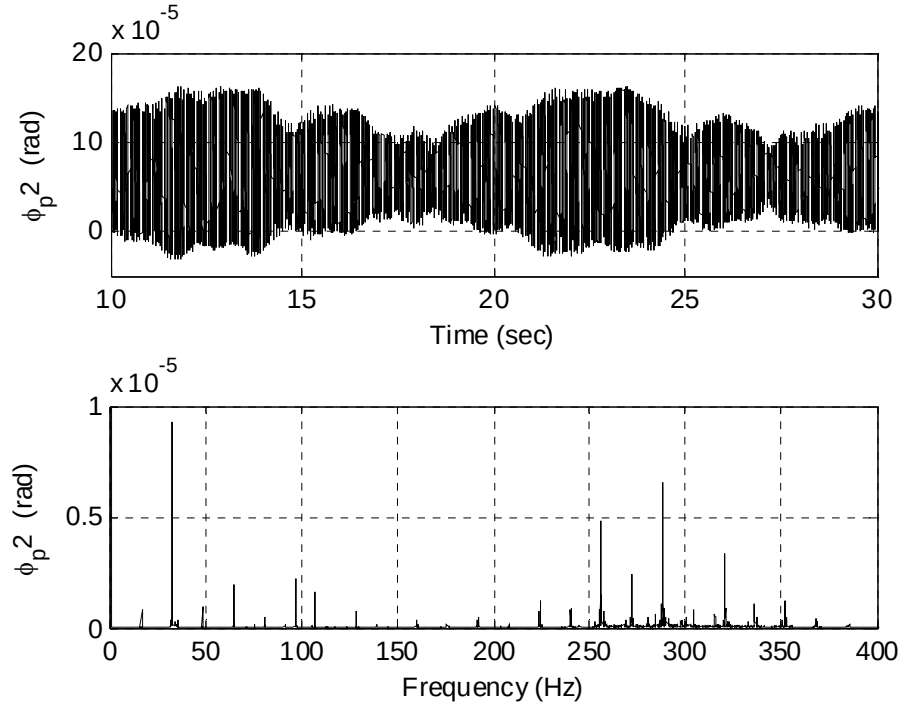

Fig. 10. *Planet 2 rotational angle* ϕ_{p2}. *From top: time series, amplitude-frequency characteristic*

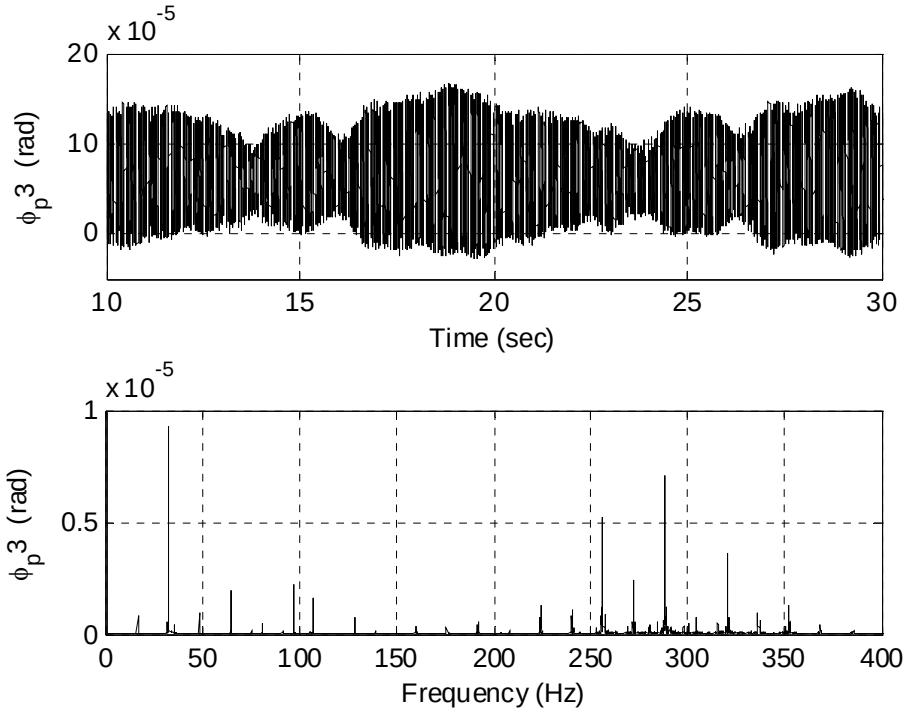

Fig. 11. *Planet 3 rotational angle* ϕ_{p3}. *From top: time series, amplitude-frequency characteristic*

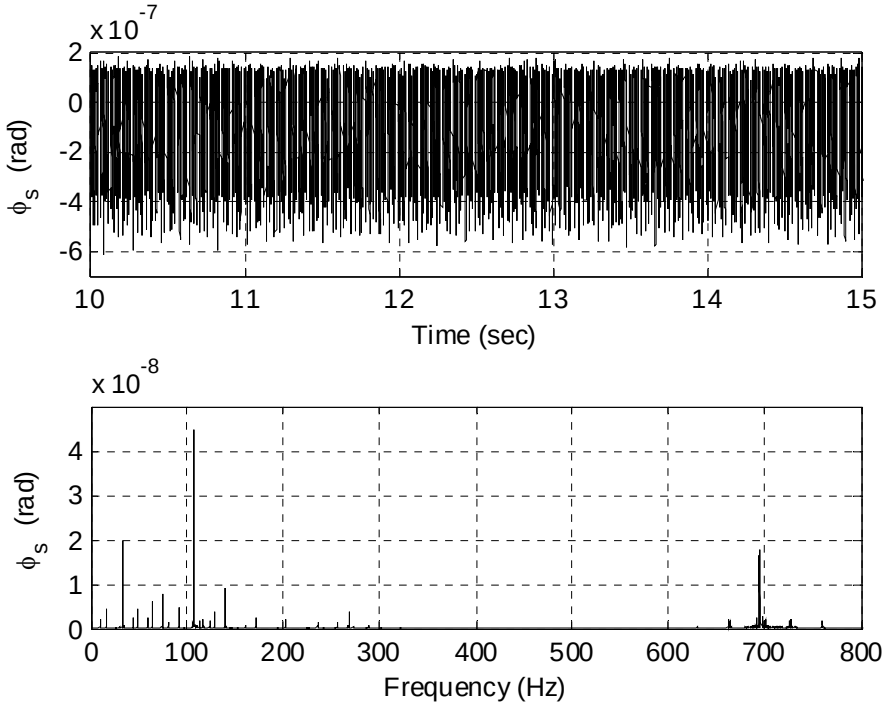

Fig. 12. *Sun rotational angle* ϕ_s. *From top: time series, amplitude-frequency characteristic*

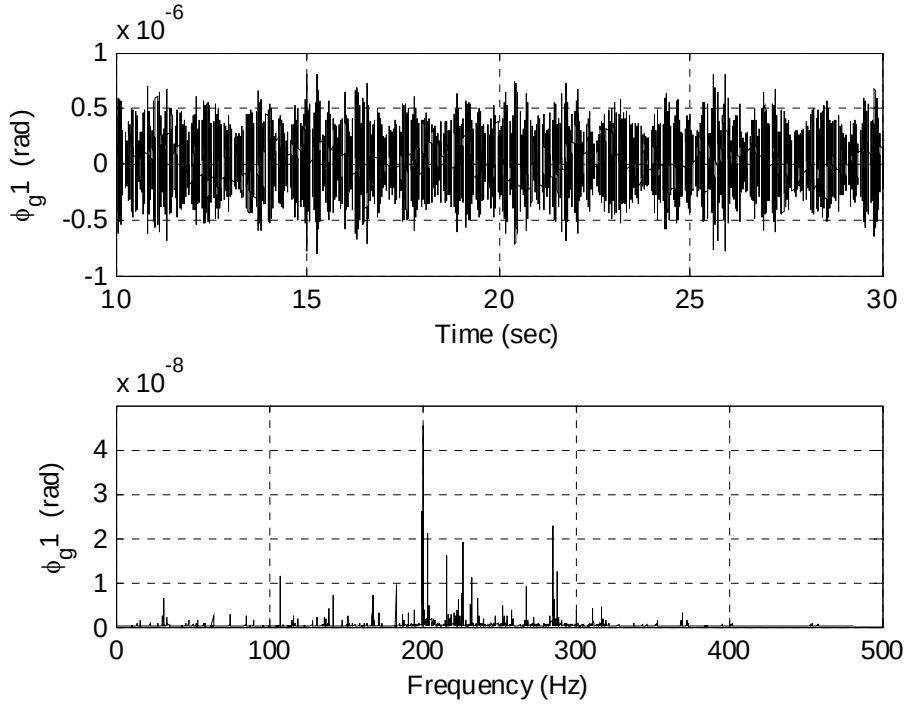

Fig. 13. *Gear 1 rotational angle* ϕ_{g1}. *From top: time series, amplitude-frequency characteristic*

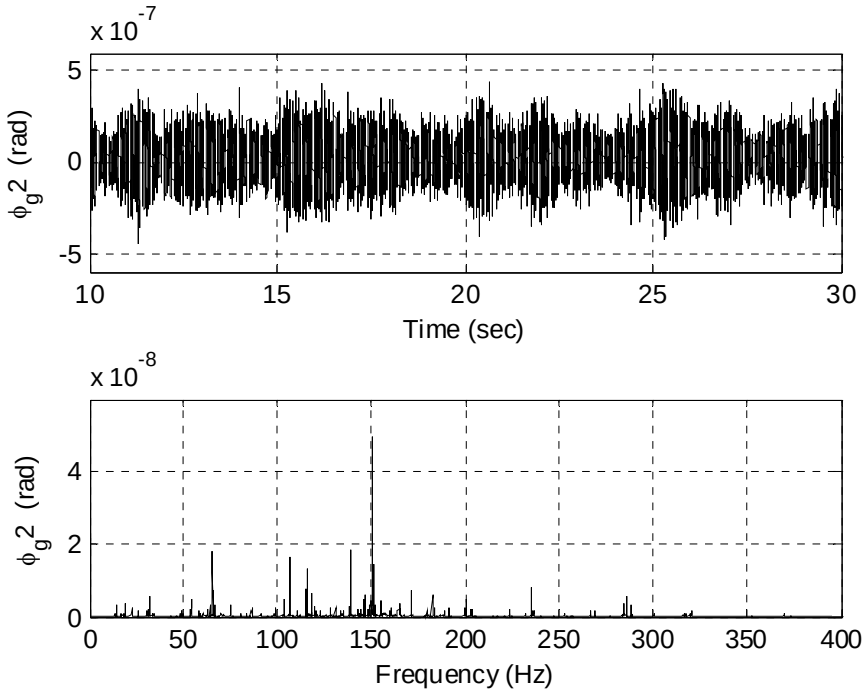

Fig. 14. *Gear 2 rotational angle* ϕ_{g2}. *From top: time series, amplitude-frequency characteristic*

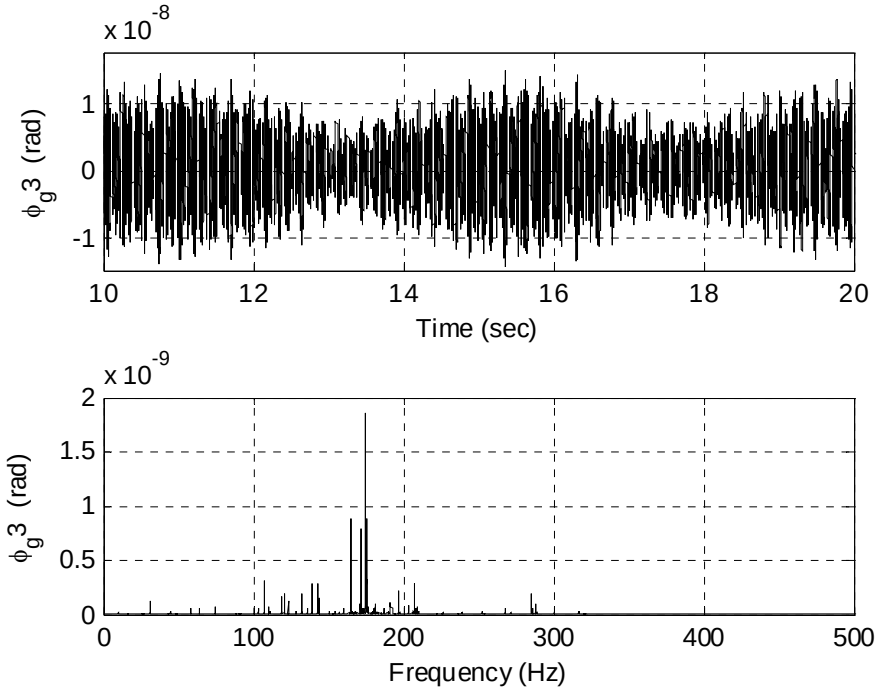

Fig. 15. *Gear 3 rotational angle* ϕ_{g3} *. From top: time series, amplitude-frequency characteristic*

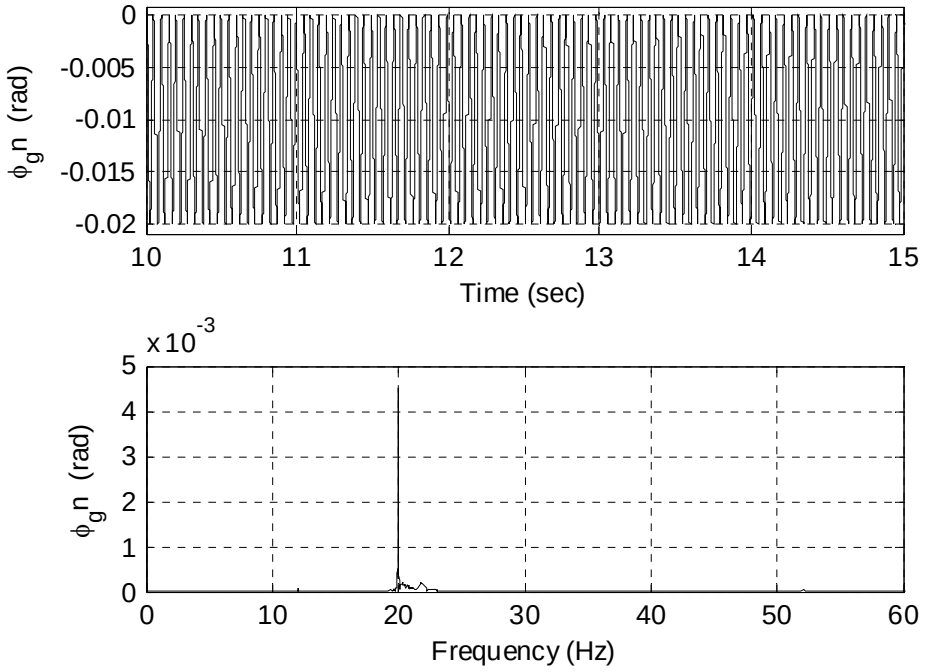

Fig. 16. *Generator rotor rotational angle* ϕ_{gn} *. From top: time series, amplitude-frequency characteristic*

4. **Conclusion and future researches**

The purpose of this article is to develop a detailed multi-body model of the wind turbine with a complex drive train.

The time series and amplitude-frequency characteristics of absolute rotation angles of the drive train parts are presented.

The analyses of the results show that there are poliharmonic vibrations in a wide range. The existence of the induced vibrations with rotation frequency and its multiplicities is connected with changeable stiffness of the gearing. Moreover, intensive parametric vibrations with frequency, which is equal to a half frequency of rotation and its multiplicities, generate themselves. In addition, the activity of vibrations of some second rate harmonics is significant and its also commensurable with that one of the main harmonics.

The results confirm the presence of vastly dynamic loads in the gearbox parts.

Future researches will extend the current model and will add the effects of bearing flexibilities.

Finally, it is important to validate and improve the wind turbine dynamic model by obtaining experimental measurements.

References

[1] A. Ams, M. Lorenz, G. Dunchev, I. Kralov, P. Sinapov, Investigation of dynamic loads in a two-stage cylindrical gear. Bul Trans-2010, Sozopol, September 24-26, 2009. pp 122-124 (in Bulgarian).

[2] V. Veits, M. Kolovskii, A. Kochura, Dynamics of controlled machine units. Moscow, Science, 1984 (in Russian).

[3] N. Minchev, V. Grigorov, Vibrodiagnostics of rotary and piston machines. Sofia, Technique 1998 (in Bulgarian)

[4] V. Ambarisha, R. Parker, "Suppression of Planet Mode Response in Planet Gear Dynamics Through Mesh Phasing," – J. Vibration and Acoustics, 2006, vol.128, pp.133-142.

[5] F. Amirouche, *Fundamentals of Multibody Dynamics – Theory and Applications*, Birkhäuser, Boston, 2006.

[6] A. Andersson, L. Vedmar, "A Dynamic Model to Determine Vibrations in Involute Helical Gears," J. Sound and Vibrations, 260, pp.195-212, 2003.

[7] T. Burton, D. Sharpe, N. Jenkins, E. Bossanyi, *Wind Energy Handbook*, Chichester, John Wiley & Sons, 2001.

[8] M. Coutinho, *Dynamic Simulations of Multibody Systems*, New-York, Springer-Verlag, 2001.

[9] Deutsches Institut für Normung, *Calculation of Load Capacity of Cylindrical gears*, DIN 3990, 1987.

[10] H. Dresig, U. Schreiber, "Vibration Analysis for Planetary Gears. Modeling and Multibody Simulation", Proceedings of ICMEM2005, October 26-28, 2005, China.

[11] J. Ekanayake, L. Holdsworth, N Jenkins, "Comparison of 5th Order and 3rd Order Machine Models for Doubly Fed Induction Generator (DFIG) Wind Turbines," Electric Power Systems Research, vol.67, pp.207-215, 2003.

[12] T. Fuglseth, "Modelling a 2.5 MW direct driven wind turbine with permanent magnet generator," Smøla, 5-11 June 2005.

[13] P. Gold et al, "Simulation of The Three-Dimensional Vibration Behavior of a Wind Energy Plant," SIMPACK Users Meeting 2004, Wartburg-Eisenach, 09-10.11.2004.

[14] A. Hansen, P. Sørensen, F. Blaabjerg, J. Becho, "Dynamic modelling of wind farm grid interaction," Wind Engineering, Vol. 26, No.4, pp.191-208, 2002.

[15] A. Heege, "Computation of Dynamic Loads in Wind Turbine Power Trains – DEWI Magazin," Nr.23, August 2003.

[16] A. Heege, J. Bertran, Y. Radovcic, "Fatigue Load Computation of Wind Turbine Gearboxes by Coupled Finite Element, Multi-Body System and Aerodynamic Analysis," Wind Energy, John Wiley & Sons, 2007.

[17] A. Kahraman, "Effect of Axial Vibrations on the dynamics of a helical gear pair," J. Vibration and Acoustics, 115, pp.33-39, 1993.

[18] N.V. Khang, T. M. Cau, N. P. Dien, "Modelling Parametric Vibration of Gear-Pair Systems as a Tool for Aiding Gear Fault Diagnosis", Technishe Mechanic, Band 24, Helt 3-4 (2004), pp.198-205.

[19] J. Lin, R. Parker, "Planetary Gear Parametric Instability", Gear Solution, September 2007, pp.32-45.

[20] J. Lin, R. Parker, "Analytical Characterization of the Unique Properties of Planetary Gear Free Vibration", Transaction of ASME, vol.121, July 1999, pp.316-321.

[21] J. Lin, R. Parker, "Mesh Stiffness Variation Instabilities in Two-Stage Gear Systems", Transaction of ASME, vol.124, January 2002, pp.68-76.

[22] G. Litak, M. Friswell, "Dynamics of a Gear System with Faults in Meshing Stiffness," Kluwer Academic Publishers, 2004.

[23] O. Lundvall, N. Strömberg, A. Klarbring, "A Flexible multi-body Approach for Frictional Contact in Spur Gears," J. Sound and Vibrations, 278, pp.479-499, 2004,.

[24] P. Nikravesh, *Computer-Aided Analysis of Mechanical Systems*, New Jersey, Prentice Hall, 1988.

[25] A. Parey, M. Badaoui, F. Guillet, N. Tandon, "Dynamic Modelling of Spur Gear Pair and Application of Empirical Mode Decomposition – Based Statistical Analysis for Early Detection of Localized Tooth Defect," J. Sound and Vibrations, 294, pp.547-561, 2006.

[26] R. Parker, "Natural Frequencies and Modal Properties of Compound Planetary Gears", Gear Solution, January 2008, pp.26-35.

[27] J. Peeters, D. Vandepitte, P. Sas, S. Lammens, "Comparison of analysis techniques for the dynamic behaviour of an integrated drive train in a wind turbine," Proc. of ISMA, vol.III, pp.1397-1405, 2002.

[28] J. Peeters, D. Vandepitte, P. Sas, "Analysis of Internal Train Dynamics in a Wind Turbine", Wind Energy, vol.9, pp.141-161, 2006.

[29] J. Peeters, D. Vandepitte, P. Sas, "Flexible multibody model of a three-stage planetary gearbox in a wind turbine," Proc. ISMA, pp.3923-3941, 2004.

[30] J. Peeters, "Simulation of Dynamic Drive Train Loads in a Wind Turbine," Katholieke Universiteit Leuven, Juni 2006.

[31] B. Rabelo, W. Hofman, M. Tilscher, A. Basteck, "A New Topology for High Powered Wind Energy Converters," EPE-PEMC'2004.

[32] G. Ramtharan, N. Jenkins, O. Anaya-Lara, E. Bossanyi, "Influence of Rotor Structural Dynamics Representations on the Electrical Transient Performance of FSIG and DFIG Wind Turbines," Wind Energy, John Wiley & Sons, 2007.

[33] P. Rosas, "Dynamic Influences of Wind Power on the Power System," Ørsted, March 2003.

[34] A. Shabana, *Dynamics of Multibody Systems*, New York, Cambridge University Press, 2005.

[35] L. Shi, Z. Hu, J. Hao, Y. Ni, "Modelling Analysis of Transient Stability Simulation with High Peneration of Grid-connected Wind Farms of DFIG Type," Wind Energy, John Wiley & Sons, 2007.

[36] B. Shlecht, T. Shulze, "Simulation of Drive trains in Wind Turbine with SIMPACK" SIMPACK Users Meeting 2003, Freiburg im Breisgau, 08-09.04.2003.

[37] B. Shlecht, T. Shulze, T. Hähnel, "Multibody-System-Simulation of Wind Turbines for Determination of Additional Dynamic Loads," SIMPACK Users Meeting 2004, Wartburg-Eisenach, 09-10.11.2004.

[38] B. Shlecht, T. Shulze, T. Rosenlocher, "Simulation of Heavy Drive Trains with Multimegawatt Transmission Power in SimPACK," SIMPACK Users Meeting 2006, Kurhaus in Baden-Baden, 21-22.03.2006.

[39] P. Sørensen et al., "Simulation and Verification of Transient Events in Large Wind Power Installations," Rizø National Laboratory, Roskilde, October 2003.

[40] S. Theodossiades, S. Natsiavas, "Periodic and Chaotic Dynamics of Motor-Driven Gear-Pair Systems with Blacklash", Chaos, Solutions and Fractals, 12 (2001), pp.2427-2440.

[41] M. Todorov, G. Vukov, I. Dobrev, "A Dynamic Multibody Model for Determination of the Torsional Vibration of the Wind Turbine," J. Machine Mechanics, v.2, pp.32-35, 2007.

[42] M. Todorov, I. Dobrev, F. Massouh, "Analysis of Torsional Oscillation of the Drive Train in Horizontal Axis Wind Turbine", Electromotion-2009, EPE Chapter Electric Drives, 2-3 July 2009, Lille, France, pp.1-7

[43] L. Vedmar, A. Andersson, "A Method to Determine Dynamic Loads on Spur Gear Teeth and on Bearings," J. Sound and Vibrations, 267, pp.1065-1084, 2003.

[44] H. Vinayak, R. Singh, "Multi-Body Dynamics and Modal Analysis of Compliant Gear Bodies," J. Sound and Vibrations, 210(2), pp.171-214, 1998.

[45] VOITH, "WinDrive®-A New Drive Train Concept for Wind Turbine," SIMPACK Users Meeting 2006, Kurhaus in Baden-Baden, 21-22.03.2006.

[46] J. Wittenburg, *Dynamics of Systems of Rigid Bodies*, Stuttgard, B.G. Teubner 1977.

[47] J. Wojnarowski, V. Onishchenko, "Tooth Wear Effect on Spur Gear Dynamics," Mechanics and Machine Theory, 38, pp.161-178, 2003.

[48] C. Yuksel, A. Kahraman, "Dynamic Tooth Loads of Planetary Gear Sets Having Tooth Profile Wear," Mechanics and Machine Theory, 39, pp.695-715, 2004.

[49] J. Zakrajesek, "Comparison of Gear Dynamics Computer Programs at NASA Lewis Research Center," NASA Technical Paper 2901, 1989.